

RESEARCH ARTICLE

Evaluation of the accuracy of soft computing learning algorithms in performance prediction of tidal turbine

Shahab S. Band^{1,2}  | Pezhman Taherei Ghazvinei³  | Khamaruzaman bin Wan Yusof⁴ |
Mohammad Hossein Ahmadi⁵  | Narjes Nabipour² | Kwok-Wing Chau⁶

¹Future Technology Research Center, National Yunlin University of Science and Technology, Douliou, Taiwan, R.O.C.

²Institute of Research and Development, Duy Tan University, Da Nang, Viet Nam

³Young Researchers and Elite Club, Shahr-e-Qods Branch, Islamic Azad University (IAU), Tehran, Iran

⁴Civil and Environmental Engineering Department, Universiti Teknologi PETRONAS, Perak, Malaysia

⁵Faculty of Mechanical Engineering, Shahrood University of Technology, Shahrood, Iran

⁶Department of Civil and Environmental Engineering, Hong Kong Polytechnic University, Hong Kong, China

Correspondence

Mohammad Hossein Ahmadi, Faculty of Mechanical Engineering, Shahrood University of Technology, Shahrood, Iran. Narjes Nabipour, Institute of Research and Development, Duy Tan University, Da Nang 550000, Viet Nam.
Email: narjesnabipour@duytan.edu.vn

Abstract

Marine renewable energy has made significant progress in the last few decades. Even after making substantial progress, the cost of electricity produced by tidal turbines is high. Therefore, the current paper concentrated on reducing the cost of transportation and installation of the turbine by performing a model. Extreme Learning Machine and Support Vector Machines as well as Genetic Programming were applied to predict the performance of the turbine model by creating short-term, multistep-ahead prediction models to compute the performance of the H-rotor vertical axis Folding Tidal turbine. The performance of the turbine was verified by a numerical study using the three-dimensional approach for the viscous model with the unsteady flow. Statistical evaluation of the outcomes pointed out that advanced Extreme Learning Machine simulation made the assurance in formulating an innovative forecasting strategy for investigating the performances of the tidal turbine. This study shows that the application of the new procedure resulted in confident generality performance and learns faster than orthodox learning algorithms. In conclusion, the assessment indicated that the advanced Extreme Learning Machine simulation was capable as a promising alternative to existing numerical methods for computing the coefficient of performance for turbines.

KEYWORDS

co-efficient of performance, extreme learning machine, folding tidal turbine, genetic programming, support vector machines, tidal current turbine

1 | INTRODUCTION

Theoretically, the ocean has the potential to generate 20,000 TWh to 92 000 TWh of electricity. While as of 2012, our planet only requires 16 000 TWh of electricity.^{1,2} A large portion of the marine energy continues to be unexploited because of the high cost involved in generating electricity.^{3,4}

Tidal current or tidal stream technologies had great strides improvement on the way to commercialization in the last decade. Tidal range technologies utilize a barrage to produce power from the elevation variance among low and high tide. The innovations made for tidal range power generation are tidal “reefs,” “lagoons,” and “fences,” as well as low head tidal barrages.⁵ There are three groups of tidal energy technologies:

This is an open access article under the terms of the Creative Commons Attribution License, which permits use, distribution and reproduction in any medium, provided the original work is properly cited.

© 2020 The Authors. *Energy Science & Engineering* published by the Society of Chemical Industry and John Wiley & Sons Ltd.

- Tidal barrage: Tidal barrage marks apply to the tides' potential energy. A tidal barrage is commonly a dam, constructed through a bay or river mouth that meets a tidal range. Tidal barrages can be classified into two categories: single basin structures and dual basin structures.⁶
- Tidal current technology presented more than 40 new devices from 2006 to 2013. The turbines are the main distinctions, which are founded on a horizontal or vertical axis.⁷
- The turbines are proportional to projects applied for wind turbines, but attributable to the upper water density smaller blades are used with more gradually and turning than wind turbines.⁸
- Responding procedures were generated by hydrofoils blades. The blades are like airplane wings to move up and down according to the tidal stream flows. Therefore, there is no need for the blade length to be constrained utilizing water depth.⁹
- The final category, Hybrid presentations are figures of tidal range technologies that have remarkable potential. The design and arrangement can be joint with the positioning and plant of a new structure in coastal regions.¹⁰

Initial investigations suggest that various factors such as fabrication, structural stability, assembly, commissioning, installation, and transportation are responsible for the high cost of per unit power.^{11,12} Recently propose the concept of Folding Tidal turbine (FTT) reduces the cost involved in the installation and transportation. FTT makes the transportation and installation easy as it has foldable parts of the shaft, blades, outer box, and connecting rods. Figure 1 illustrates the diagram of the vertical and horizontal axis FTT. This study investigates only the vertical axis FTT. However, the proposed FTTs are designed to have both the vertical and horizontal axes. Lam et al discuss the parts of FTT, specifications of the material, and installation process of FTT.¹³ A system nonlinearities and parametric uncertainties were applied to model a hydrostatic tidal turbine (HTT) model associated with hydrostatic dynamics. An ELM based nonlinear was considered to realize sensor-less remarks of turbine torque and tidal stream speeds. The projected proposal, modeling,

and controller of the HTT were validated by virtual reality with the credible Simulink/Simscape. It was indicated that the suggested controlling systems reached considerably superior performance than the proportional-integral-derivative regulator.¹⁴ According to the data-driven wind farm interpreter, a reserved problematic optimization was communicated by designing a multi-objective predictive controller. Outcomes showed that the wind farm thrust was reduced up to 12.96% even though the wind farm power generation can be sustained at practically a similar level by using the same control in comparison with a forecasting conventional control model.¹⁵ Recently, an adaptive backstepping controller with improbability and disturbance estimate was suggested to take full advantage of a generic horizontal marine turbine. The turbine was modeled for controlling implementation. The problematic regulator was verbalized and the controller was designed based on the self-possessed of the turbine speed looping control as well as the q-axis current. Simultaneously, the disturbance and uncertainty were predicted and recompensed in the control. The performance was compared with a conventional backstepping controller. The results specified that the suggested control was freely superior in improving the efficiency of the power generation in the same condition than conventional control. The turbine generates more power (up to 30%) by using proposed control than that with the conventional control.¹⁶

There are two types of tidal turbines: horizontal axis and vertical axis, depending on the orientation of the rotor shaft. The horizontal axis turbines have higher efficiency than vertical axis turbines.^{17,18} Therefore, the horizontal axis turbines are popular in the wind energy and tidal current energy sector.^{19,20} Nevertheless, studies suggest that both the vertical and horizontal axis turbines have advantages and drawbacks over each other. Therefore, engineers determine the suitable design of the turbine by investigating the requirements of the installation site. The main advantages of vertical axis turbines are better compactness, comparatively low cost due to the simple structure, absence of yaw-control mechanism, high per square meter power density due to placement of the turbines closer to each other and housing of "electrical" and

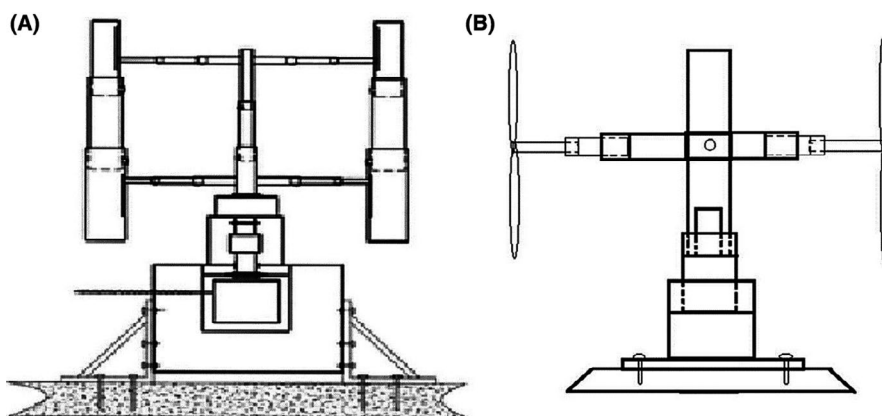


FIGURE 1 Schematic diagram of (A) Vertical Axis and (B) Horizontal Axis FTT

"mechanical" components, gearbox and generator at the base. Alternatively, the major drawbacks of the turbines with vertical axis are that they are not self-starting, have low efficiency, and produce larger shaft bending moment which leads to failure or fracture of shaft and bearings.

This study uses the H-rotor vertical axis FTT. It has better features like the straightforward blades, which are straight linked to the shaft. Also, the H-rotor is capable of producing power by intercepting water flow from all directions, easy to install, build, and maintain which lowers the cost of power production.²¹

Current research proposed using a simplified approach for projecting the coefficient of performance of tidal turbine using soft computing procedures. Researchers need to study the performance of FTT for various types of blades with the aim of progress their performance. Therefore, estimating the performance of FTT is a key point in optimizing the blade shape for better efficiency. Accurate estimation of FTT's performance will help in reducing the cost involved in the physical experiments (physically designing FTT by trial and error). It will also help to forecast the range of tip speed ratio (TSR) in which the FTT achieves optimum efficiency.

The manuscript comes up with an in-depth study of the efficiency calculation by using hydro-dynamic methods (by using Fluent 6.1 and Gambit 2.2.30) followed by the machine learning approach methods to forecast the FTT performance. A review of the literature showed the prediction of the power plant condenser performance and forecasting the tidal energy by using a numerical method.²² Moreover, similar three-dimensional models were used to predict the turbine's performance^{20,23}; estimating performance of turbines; predicting long-term tides; and tidal elevation and wind power generations, respectively.^{17,22,24,25}

Equation (1) describes the calculation parameters of the performance coefficient²⁴:

$$C_p = 0.5\rho AV^3, \quad (1)$$

where C_p is the coefficient of performance (dimensionless), ρ is the water density (kg/m^3), A indicates the contact area (m^2) to incoming flow, besides V is the inlet velocity (m/s) of water. In the case of a vertical axis turbine, the interaction area to incoming flow is the product of turbine height and rotor diameter. The number of rotations a turbine makes in one minute also affects the calculations while doing numerical simulations. Hence, TSR (dimensionless) is introduced which is given by Equation (2).²⁶

$$TS = \omega R / V, \quad (2)$$

where ω stands for rotational speed (in rpm), R points to the turbine radius, and V specifies the inlet velocity as mentioned before. Hence, all these parameters are necessary for predicting

the performance of the turbine. Besides, outcome results from the fluent simulations are sensitivity to the choice of a time step. Therefore, this study considered four income variables, that is, TSR, turbine area, air density, and station visibility.

Numerical approaches are being extensively applied because of the improved precision compared to the empirical solutions. Numerical methods involve compound environment parameters for modeling the performance of tidal turbines, accurately. Nevertheless, even the numerical method's correctness depends on income data. Numerical approaches include high computation source and compound exogenous variables. Consequently, the need for a simpler and accurate process for forecasting the coefficient of performance of tidal existing turbines was the initials of the current research. The literature review showed that a multi-objective forecasting frame had been examined in forecasting the wind farm power harvest. The forecasting frame applied the average wind farm production and the correspondent thrust of the turbine utilizing the reaction variables and the wind circumstances, controller sets, and turbine features in place of forecaster variables. The simulations were consequently created through five data excavating procedures containing RF, GRNN, GBR, RNN, and SVM. The forecasting performances of the procedures were evaluated based on the latest version of FLORIS. The results confirmed that all the procedures achieved the qualified precision equal to or more than 99%. The RNN revealed a higher accuracy than the and particularly the others.²⁷

Despite recent developments, the potential of other algorithms for data-driven the performance of Tidal Current Turbines has never been mined. Consequently, the leading objective of current research work was methodically set to evaluate more numerical approaches for computing coefficient of performance of tidal turbine applying Extreme Learning Machine (ELM), Support Vector Machines (SVM), and Genetic Programming (GP). Neural Network (NN) as the main computing simulator was used widely in several engineering subjects. NN solves compound nonlinear difficult complications, which cannot be answered by the classic approaches.²⁸⁻³⁰ Unseen Markov Mockup (HMM), support vector machine (SVM), and backpropagation are the numbers of commonly used methods algorithms in training the neural network. The NN defect is its requirement for a longer learning period within the Extreme Learning Machine (ELM) as the NN sole layer feeder.³¹ NN solves problems of gradient descent according to procedures like backpropagation where ELM decreases the required training period for the Neural Network. In reality, utilizing ELM approved that this learning algorithm is fast to generate accurate performance.^{17,32-37}

The processes of statistical machine learning along with minimization of structural risk were considered in establishing the SVM. These ensure the minimization of the upper guaranteed generality error rather than limited

training error. The latter is a collective attitude preferred over many other conventional machine learning systems.³⁸ This evaluated a predictive model using ELM, SVM, and GP methods for estimating the coefficient of performance for tidal turbines.

2 | METHODOLOGY

2.1 | Data acquisition

Among all the parts of the tidal current turbine, the role of the blade is crucial. It transforms the energy of the water from kinetic to rotational. The geometry of the turbine blades effects the efficient working and stability of the turbine. Studies have shown that if the rotations per minute of the machine are fixed then the area under the graph plotted between the power coefficient (C_p) (y-axis) and tip speed ratio (x-axis) gives the power captured by that turbine.³⁹

The coefficient of performance was first computed by running numerical simulations by using Fluent 6.1. The geometry of the foldable bladed turbine was created by using Gambit 2.2.30, and numerical calculations were made by running a three-dimensional simulation. This study inherited the geometry of straight-bladed of the vertical axis tidal recent. However, there are few changes inherited compared to the aforementioned studies. This study uses three-bladed turbines with each blade having three foldable parts. The chord length and height of the bottom-most part are 160 and 260 mm, respectively. Later, the ratio of 0.95 was followed for the middle part, and again, the top-most part is 0.95 times smaller than the middle part of the blade. The overlapping of each blade entity with another is 10% of the smaller blade height. The hydrofoil of the blade is NACA 0025 and the radius of the turbine is 450 mm as used in this study (Figure 2).

2.2 | Income and outcome variables

As explained in the aforementioned sections to investigate the performance of FTT, C_p was calculated at various water velocities. Table 1 illustrates the description and values of the income data.

3 | SOFT COMPUTING LEARNING ALGORITHMS

3.1 | ELM

ELM was announced to act as a learning system in single layer feeding of the neural network (SLFN)

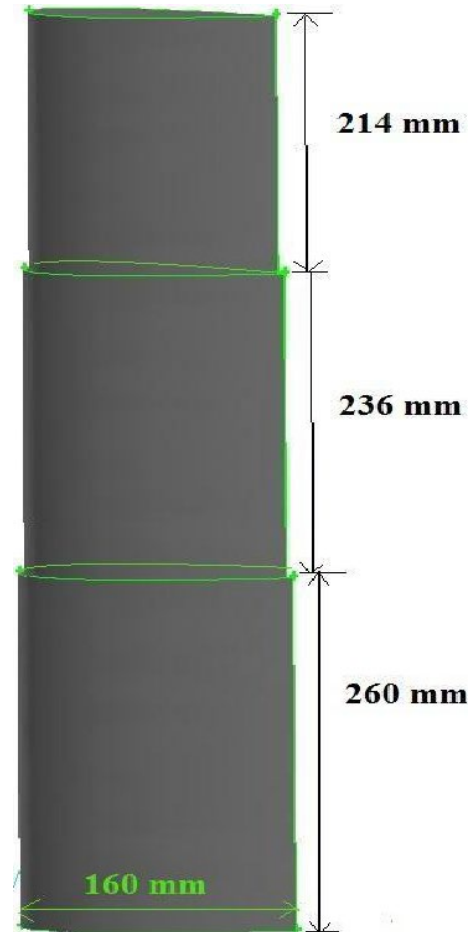


FIGURE 2 Design of FTT blade created by using Gambit 2.2.30

architecture.⁴⁰⁻⁴² ELM arbitrarily picks out the income weightiness then calculates SLFN's outcomes weightiness. As an ELM proficient algorithm using frequent benefits such as accessibility, superior performance, faster tutorial, suitable for nonlinear kernel and activation functions.^{43,44} Besides better performance, ELM is an influential procedure with quicker tutorial speed and associated with customary procedures like backpropagation (BP). BP analytically regulates the network factors, thereby averting manual interventions for trivial issues.

3.1.1 | Single unseen layer feed-forward NN

The mathematical description of SLFN incorporates both additive plus RBF unseen nodes. It represents the functions of SLFN with L unseen nodes⁴⁵⁻⁴⁷:

$$f_L(x) = \sum_{i=0}^L \beta_i G(a_i, b_i, x), \quad x \in R^n, \quad a_i \in R^n, \quad (3)$$

where β_i specifies the weight for a connection concerning the i th unseen and outcome, a_i and b_i indicate the tutorial

TABLE 1 Income variables for the calculation of coefficient of performance for FTT

Incomes	description	characterization
Income 1	TSR (Dimensionless)	turbine inlet velocity, rotation per minute is fixed at 60 rpm
Income 2	Area (m ²)	vertical axis turbine it is the multiplication of blade height with the turbine diameter)
Income 3	Density (kg/m ³)	Describes the medium in which the turbine is working
Income 4	Time Step (seconds)	Time duration defined in Fluent to record the outcome

parameters for i th unseen nodes. Besides, $G(a_i, b_i, x)$ directs the i th node outcome in place of income x . The preservative unseen node through the stimulation purpose of $g(x): R \rightarrow R$ (eg, Sigmoid and threshold), $G(a_i, b_i, x)$ is ⁴⁸ as follows: $G(a_i, b_i, x) = g(a_i \cdot x + b_i)$, $a_i \in R$,

where x is the inner product of two vectors a_i also x in R^n . The RBF unseen node per initiation function $g(x): R \rightarrow R$ (eg, Gaussian), obtains $G(a_i, b_i, x)$ using Equation (5).⁴⁸

$$G(a_i, b_i, x) = G(b_i ||x - a_i||), \quad b_i \in R, \quad (4)$$

a_i in addition to b_i characterizes the midpoint and impression factor of i th RBF node. R^+ specifies a set of real positive values. RBF network can be reflected as a particular case of SLFN, where SLFN unseen layers have RBF nodes Consider $(x_i, t_i) \in R^n \times R^m$ represents randomly selected N separate samples, where x_i is income vector of size $n \times 1$, besides t_i is the object vector with the of size $m \times 1$. Whenever SLFN estimates the N -samples with 100 percent accuracy:

$$fL(x_j) = \sum_{i=1}^L G(a_i, b_i, x_j), \quad j = 1, \dots, N. \quad (5)$$

Equation (7) is a short form of Equation (6):

$$H\beta = T, \quad (6)$$

where

$$H(\tilde{a}, \tilde{b}, \tilde{x}) = \begin{bmatrix} G(a_1, b_1, x_1) \cdots G(a_L, b_L, x_1) \\ \vdots \\ G(a_1, b_1, x_N) \cdots G(a_L, b_L, x_N) \end{bmatrix}_{N \times L} \quad (7)$$

with $\tilde{a} = a_1, \dots, a_L$; $\tilde{b} = b_1, \dots, b_L$; $\tilde{x} = x_1, \dots, x_L$

$$\beta = \begin{bmatrix} \beta_1^T \\ \vdots \\ \beta_L^T \end{bmatrix}_{L \times m} \quad \text{and} \quad T = \begin{bmatrix} t_1^T \\ \vdots \\ t_L^T \end{bmatrix}_{N \times m}, \quad (8)$$

where H directs the outcome matrix of the unseen SLFN layer. The i th column of H being the outcome of i th -unseen node for incomes x_1, \dots, x_n .

3.1.2 | Attitude of ELM

ELM is considered in place of an SLFN within the unseen neurons for tutoring L individual trials by nil error.⁴⁹ In the case of the fewer unseen neurons (L) toward the number of individual trials (N), ELM still allocates arbitrary factors to the unseen nodes. It also calculates the outcome weightiness by the inverse of H through only an insignificant error ϵ bigger than zero. The unseen node factors of ELM, a_i and b_i should not be adjusted in training as they straightforwardly allocate by random values as indicated below.

Proposition 1 Specified a substantially differentiable SLFN in an interval R has L stabilizer or RBF unseen nodes besides an initiation task $g(x)$.⁴⁶ Formerly in place of arbitrary L separate income vectors $\{x_i | x_i \in R^n, i = 1, \dots, L\}$ besides $\{(a_i, b_i)\}_{i=1}^L$ formed arbitrarily by any constant prospect scattering, correspondingly. The outcome matrix of the unseen layer is invertible with possibility one, the unseen layer outcome matrix H of the SLFN is invertible and $\|H\beta - T\| = 0$.

Proposition 2 Assumed every minor positive value $\epsilon > 0$ plus initiating task $g(x): R \rightarrow R$ where is substantially differentiable in every interval. For any $L \leq N$ so that for N arbitrary distinct income vectors $\{x_i | x_i \in R^n, i = 1, \dots, L\}$ intended for all $\{(a_i, b_i)\}_{i=1}^L$ arbitrarily created based on the constant possibility distribution $\|H_{N \times L} \beta_{L \times m} - T_{N \times m}\| \leq \epsilon$ with probability one.⁴⁶

In the meantime, the unseen node factors of ELM need no adjustment in training. They are straightforwardly allocated through arbitrary values. Equation 5 suits a direct arrangement besides the yield masses can be projected as ⁵⁰:

$$\beta = H^+ T, \quad (9)$$

where H^+ is the Moore-Penrose general inverse of the unseen layer yield matrix. H is calculated via quite a few methods containing orthogonal projection, or the simplification, iterative, singular value decomposition (SVD), etc The orthogonal forecasting model is being operated only when $H^T T$ is nonsingular and $H^+ = (H^T T)^{-1} H^T$. Although orthogonalization and iterative processes have some limits, executions of ELM procedures SVD to calculate the Moore-Penrose generalized inverse of H developing in all conditions.

3.2 | SVM

SVMs or Support vector machines are an excellent soft computing learning algorithm, capable of regression analysis, prediction of result trends, classification, and recognition of the pattern. A review showed the advanced application of SVMs in hydrological and environmental computing, compared to other conventional statistical models.⁵¹ Minimization of the upper guaranteed generality inaccuracy instead of limited training inaccuracy is regarded as one of the advantages of the SVM compared to other soft computing learning process. Also, SVM provides a suitable solution owing to the convex nature of the optimal problems without the need for assumptions; SVM initiates discreetly nonlinear transformation through the kernel functions. SVM equations expressed in Equations (11-14) are based on Vapnik's theory. Assuming a data set of points is specified by $\{x_i, d_i\}_i^n$, where x_i is the input space vector of the data trial, d_i is the objective value, and n is the data dimension. SVM estimates the task as symbolized in the following equations:

$$f(x) = w\varphi(x) + b, \tag{10}$$

$$R_{SVMs}(C) = \frac{1}{2} \|w\|^2 + C \frac{1}{2} \sum_{i=1}^n L(x_i, d_i), \tag{11}$$

where $\varphi(x)$ symbolizes the extraordinary dimensional space feature which mapped the input space vector x , b : a scalar, w : a normal vector, and $C \frac{1}{2} \sum_{i=1}^n L(x_i, d_i)$ embodies the risk (empirical error). Estimation of the parameter b and w is done through diminishing the normalized risk task as shown in Equation (13). This becomes possible after introducing the positive slack variables ξ_i and ξ_i^* . These parameters signify higher and lesser excess deviation.⁵²

$$\text{Minimize } R_{SVMs}(w, \xi^{(*)}) = \frac{1}{2} \|w\|^2 + C \sum_{i=1}^n L(\xi_i, \xi_i^*), \tag{12}$$

$$\text{subject to } \begin{cases} d_i - w\varphi(x_i) + b_i \leq \varepsilon + \xi_i \\ w\varphi(x_i) + b_i - d_i \leq \varepsilon + \xi_i \\ \xi_i, \xi_i^* \geq 0, \quad i = 1, 2, 3, \dots, l, \end{cases} \tag{13}$$

where $\frac{1}{2} \|w\|^2$ represents the regularization term, C is the error penalty, ε is the loss function, and l is the number of data set used for training. Factor C regulates the variation among the regularization term and empirical error (risk). By introducing the Lagrange multiplier and optimality constraints, Equation (11) can be solved to obtain a generic function shown in Equation (15).

$$f(s, a_i, a_i^*) = \sum_{i=1}^n (a_i - a_i^*) K(x, x_i) + b, \tag{14}$$

where the kernel function $K(x, x_i) = \varphi(x_i) \varphi(x_j)$. It represents the product of the inner vectors x_i and x_j in the space $\varphi(x_i)$ and $\varphi(x_j)$, respectively.

Data correlation is one of the significant applications of SVM, and it is carried out with the nonlinear mapping performance. A nonlinear learning mechanism can be fabricated if an income withdrawal is in place of directly computing the inner product of feature space in terms of the initial inputs. This method is called a straight calculation technique of a kernel task (K). Therefore, SVM accomplishes selected kernel functions and transforms the data onto the results of higher-dimensional feature space. These SVMs' consequences agree with the outcomes of the original lower-dimensional input space.

Four elementary kernel tasks in SVM are namely the lineal, polynomial, sigmoid, and radial basis function (RBF). RBF showed the best kernel task attributable to its consistency and effectiveness in handling complex parameters. Besides, RBF has a simplicity of usage for optimization and adaptive techniques.^{53,54} RBF kernel does not need complicated quadratic programming problem but required only several linear equations for a solution.⁵⁵ Hence, RBF is adopted in this study, with the parameter. Equation (16) shows the nonlinear radial basis kernel function:

$$K(x_i, x_j) = \exp\left(-\gamma \|x_i - x_j\|^2\right), \tag{15}$$

where variable x_i and x_j are the input space vectors. These vectors comprise the features calculated after the testing or training data set.

Accuracy of the RBF forecasting highly depends on three parameters (γ, ε , and C). Grid search is the conventional approach for selecting these parameters, which involves exhaustive searching over a by hand quantified division of the hyper factor space of a learning procedure. Several performance metrics are required to guide the grid search algorithm. The firefly optimization algorithm was used in current work to catch the ideal values of these factors.

3.2.1 | SVM parameters collection by firefly enhancement procedure

Metaheuristic enhancement procedures are used widely motivated by nature in various fields of human accomplishments.⁵⁶⁻⁵⁹ Quite a few prominent instances comprise the particle swarm optimization (PSO), genetic algorithm (GA), ant colony optimization (ACO), and the cuckoo search (CS). Improvement of these procedures states to the selection appliance aimed at the appropriate in biological arrangements. Newly advanced FFA is one such biological motivated metaheuristic enhancement procedure that mimics the flashing individual of fireflies. FFA was advanced procedures the luminance construction source (bioluminescence) to permit extra firefly to pursuit the path for prey or mates.⁶⁰ The luminance construction perception advances procedures resolutions for many optimization complications. As an associate to other biological stimulated optimization procedures, the fireflies' procedure is further operative for limited and comprehensive resolutions. There are quite a lot of essential instructions in FFA improvement (a) the luminance yield or luminous concentration distress the attraction of a firefly toward alternative one. More intensity of firefly's luminance will appeal other fireflies, (b) supposition that the fireflies are unisex and capable to appeal each further irrespective of gender (c) the nature of the encoded cost task impresses the illumination, that is, the illumination is a fraction to the suitability rate or objective task.⁶¹ Two important complications exist in the improvement of FFA, which comprises origination of the objective load (attractiveness) and a variant of the bright concentration. For example, the optimal resolution for the objective task is comparative to the fitness task or the concentration of the firefly's luminance. As a result, the lower concentration of light attributable to greater space among fireflies decreases attraction to the formers. Equation (17) indicates the affiliation among light concentration and space.

$$I(r) = I_0 \exp(-\gamma r^2), \quad (16)$$

where I signifies the concentration of light at a space r from a firefly, I_0 characterizes preliminary concentration of light, where $r = 0$, and γ is a continual between 0.1 and 10 that symbolizes the light absorption coefficient.⁶² The subsequent equation is applied for stating the attractiveness β next to r from the firefly:

$$\beta(r) = \beta_0 \exp(-\gamma r^2). \quad (17)$$

The attractiveness at $r = 0$ is represented by β_0 . A specific space $T = 1/\sqrt{\gamma}$ expresses Equation (8) over which noticeable changes follow from β_0 to $\beta_0 e^{-1}$.

The Cartesian space among firefly and can be signified by Equation (19):

$$r_{ij} = \|x_i + x_j\| = \sqrt{\sum_{k=1}^d (x_{i,k} - x_{j,k})^2}. \quad (18)$$

Equation (20) symbolizes indication of when attracted to brighter firefly j .

$$\Delta x_i = \beta_0 e^{-\gamma r^2(x_j - x_i) + \alpha \epsilon_i}, \quad (19)$$

where the first term signifies the attraction, the additional term indicates the randomization; where is the coefficient of randomization ($0 \leq \alpha \leq 1$) and ϵ_i is the random number vector attained from a Gaussian distribution. Equation (11) is applied for bringing up the succeeding step of firefly's as demonstrated in Figure 3.⁶³

$$x_i^{i+1} = x_i + \Delta x_i \quad (20)$$

3.3 | Genetic programming

GP approximates the equation that describes the relationship of income variables to the outcome variables. The procedure initially contemplates a primary population consisting of randomly produced equations. It chooses combinations of income variables, tasks, and constant numbers, based on initial awareness of a given problem, randomly. It also includes arithmetic and logical operators, trigonometric and algebraic functions.

The populations of potential equations (program) are exposed to a transformative route. Here, the "fitness" of the equation is valued to see in what manner fighting fit they answer the given problem. GP chooses the equations that superlative are best fit for the given problem. Further better programs are chosen from the selected set by "crossover" and "mutation" to simulate the natural world's imitation procedure. In the crossover, portions of the preeminent platforms are exchanged. During mutation, new programs are generated by randomly changing parts of selected programs. Naturally, equations (programs) which less fit the data are excluded from the set of solution. These steps are repeated over successive generations to find an equation that describes the relationship of income variables to the outcome variables.^{64,65}

3.4 | Input and output variables

The theory of performance prediction was explained in the previous section. The parameters of flow contact area, velocity (tip speed ratio), and density of the medium had significant impacts on the turbine performance. However, the time step at which the output was recorded by the Fluent also played a vital role. The lower time steps had better accuracy. Therefore, the time

\Firefly Algorithm

```

start
  Define the objective function,  $f(x), x = (x_1, \dots, x_d)^T$ 
  Generate initial population of fireflies  $x_i (i = 1, 2, \dots, n)$ 
  Determine light intensity  $l_i$  at  $x_i$  from  $f(x_i)$ 
  Define light absorption coefficient  $\gamma$ 
  while  $t < \text{Max Generation}$ 
    Make a copy of population for movement function
    for  $i = 1:n$  all  $n$  fireflies
      for  $j = 1:i$  all  $n$  fireflies
        if  $(l_j > l_i)$ 
          Move fireflies  $i$  and  $j$  in  $d$ -dimension;
        end if
        Attractiveness varies with distance  $r$  via  $\exp[-\gamma r]$ 
        Evaluate new solution and update light intensity
      end
    end
    Rank the fireflies and find the current best

  Post process results and visualization
end
  
```

FIGURE 3 Pseudo-code for Firefly Algorithm

Inputs	Parameters description	Parameter characterization
1	Area (m ²)	The flow contact area (for the vertical axis turbine, it is the multiplication of blade height with the diameter of the turbine)
2	Time step (seconds)	Time duration defined in Fluent to record the output
3	Tip speed ratio (Dimensionless)	The inlet velocity for the turbine, the rotation per minute was fixed at 60 rpm
4	Density (kg/m ³)	Describes the medium in which the turbine is working

TABLE 2 Input parameters for calculating the coefficient of performance

step chosen for recording the output was also taken as an input parameter for the soft computing procedures. Table 2 defines the parameters used for calculating the Cp.

$$r = \frac{n (\sum_{i=1}^n O_i \times P_i) - (\sum_{i=1}^n O_i) \times (\sum_{i=1}^n P_i)}{\sqrt{(n \sum_{i=1}^n O_i^2 - (\sum_{i=1}^n O_i)^2) \times (n \sum_{i=1}^n P_i^2 - (\sum_{i=1}^n P_i)^2)}} \tag{22}$$

4 | RESULTS AND DISCUSSION

4.1 | Evaluation

Forecasting presentations of projected simulations were measured to train and test data set. The statistical factors were root means square error (RMSE), Pearson coefficient (r), and Coefficient of determination (R^2).

$$RMSE = \sqrt{\frac{\sum_{i=1}^n (P_i - O_i)^2}{n}} \tag{21}$$

$$R^2 = \frac{\left[\sum_{i=1}^n (O_i - \bar{O}) \cdot (P_i - \bar{P}) \right]^2}{\sum_{i=1}^n (O_i - \bar{O}) \cdot \sum_{i=1}^n (P_i - \bar{P})} \tag{23}$$

where O_i and P_i are the heat load from the forecast and experiment in turn, where n stands for the data number of the test.

4.2 | Methods' performance

This section reports the ELM results for the coefficient of performance for the tidal turbine projecting model. Figure 4A illustrates the precision of the advanced ELM coefficient for the performance of the proposed tidal turbine. It was found that the significant number of the points drop horizontally the diagonal line in ELM forecasting simulation. Thus, the estimation is in the significant agreement using the observed values for the ELM process with an extraordinary coefficient of determination against a few overestimated or underestimated values. Besides, Figure 4B shows the accuracy of advanced SVM-FFA Cp for the FTT

projecting model. Moreover, the furthermost of the points fall alongside the diagonal line for the SVM-FFA forecast model. Accordingly, it tracks that forecast outcome have a good arrangement with the measured amounts for the SVM-FFA technique. This statement is maintained with the actual extraordinary value of R^2 and with the parts of overestimated or underestimated amounts. As a result, it is noticeable that the forecast values are at satisfactory level accuracy. Next, Figure 4C illustrates the accuracy of the advanced GP forecasting model. It demonstrates that the furthermost of the points accompanied by the diagonal are in line with GP forecasts. Therefore, it tracks that forecast outcome with close the measured values for the GP

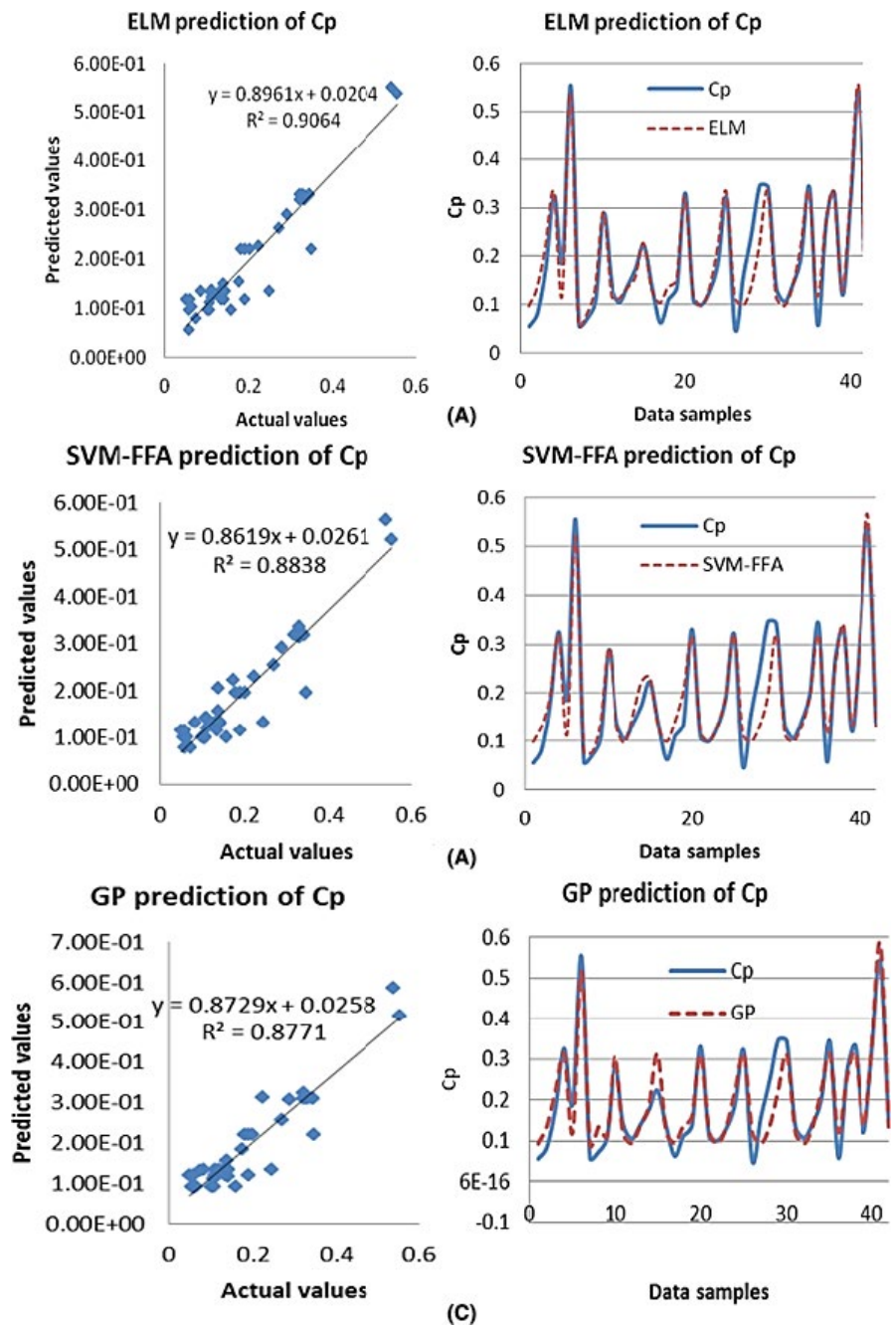


FIGURE 4 Scatters of real and forecast amounts of Cp for FTT by using (A) ELM, (B) SVM-FFA, and (C) GP process

TABLE 3 Statistics indicators for the procedures' outcome

Method	Parameter		
	RMSE	R^2	r
ELM	0.037	0.90	0.95
SVM-FFA	0.042	0.88	0.94
GP	0.043	0.87	0.93

technique although there are negligibly overestimated or underestimated values.

4.3 | Evaluation of the ELM, SVM-FFA, and GP

The turbine shows the highest performance of 0.554 at the TSR of 1 with the flow contact area of 0.525 m². However, the lowest performance was predicted at the TSR of 3.76 with the flow contact area of 0.639. In determining the assets of the ELM method on a further confident and perceptible source, ELM models' were evaluated with GP and ANN approaches in forecasting accuracy. Table 3 indicates the ELM model outperforms SVM-FAA and GP simulations. RMSE analysis indicated that the projected ELM exceeded the outcomes found through the point of reference simulations.

5 | CONCLUSION

The concept of FTT was proposed to bring down the cost of transportation and installation. This study investigated the performance of the H-rotor vertical axis Folding Tidal turbine using Extreme Learning Machine and Support Vector Machines as well as Genetic Programming by creating short-term, multistep-ahead prediction models. The performance of the turbine was verified by a numerical study using the three-dimensional approach for the viscous model with the unsteady flow. The coefficient of performance was first calculated by using Fluent 6.1, and the outcomes were evaluated using the predicted amounts obtained by the ELM approach. The inlet velocity and inlet flow contact area were varied in the calculation of the turbine performance. On average, it was observed that the performance improves with the increase in TSR, and after a maximum value, it starts depreciating. The research conducted a systematic methodology to generate the ELM coefficient of performance of the tidal turbine forecasting process. ELM process was evaluated by SVM-FAA and GP to assess the forecasting precision by the RMSE, r , and R^2 indicators. The statistical evaluation indicated that ELM forecasts were more robust also accurate than the other techniques in RMSE and r , by 11% improvement. It was found that

unlike the traditional learning procedures the ELM gave a minimum error in addition norm of the masses. Moreover, the significant features of the advanced ELM simulation made it different from the other gradient-based procedures.

ACKNOWLEDGMENT

The authors wish to extend their gratitude to the Ministry of High Education for their financial support under UM/MOHE High Impact Research Grants no UM.C/HIR/MOHE/ENG/34 and UM.C/HIR/MOHE/ENG/47.

ORCID

Shahab S. Band  <https://orcid.org/0000-0002-8963-731X>

Pezhman Taherei Ghazvinei  <https://orcid.org/0000-0001-9186-7109>

Mohammad Hossein Ahmadi  <https://orcid.org/0000-0002-0097-2534>

REFERENCES

1. Esteban M, Gasparatos A, Doll CN. Recent Developments in Ocean Energy and Offshore Wind: Financial Challenges and Environmental Misconceptions. *Sustainability Through Innovation in Product Life Cycle Design*. Springer; 2017:735-746.
2. Pelc R, Fujita RM. Renewable energy from the ocean. *Marine Policy*. 2002;26(6):471-479.
3. Elghali SB, Benbouzid M, Charpentier JF. Marine tidal current electric power generation technology: State of the art and current status. In *2007 IEEE International Electric Machines & Drives Conference*. 2007. IEEE.
4. Ponta F, Jacovkis P. Marine-current power generation by diffuser-augmented floating hydro-turbines. *Renewable Energy*. 2008;33(4):665-673.
5. Henriksen M, Piccioni SDL, Lai M. New Combined Solution to Harness Wave Energy—Full Renewable Potential for Sustainable Electricity and Fresh Water Production. In *Multidisciplinary Digital Publishing Institute Proceedings*. 2019.
6. Rourke FO, Boyle F, Reynolds A. Tidal energy update 2009. *Appl Energy*. 2010;87(2):398-409.
7. Watson J, Gross R, Ketsopoulou I, Winkler M. UK energy strategies under uncertainty: synthesis report. 2014.
8. Michalena E, Hills JM. Paths of renewable energy development in small island developing states of the South Pacific. *Renew Sustain Energy Rev*. 2018;82:343-352.
9. Haas KA, Yang X, Fritz HM. Modeling impacts of energy extraction from the Gulf Stream System. 2014.
10. Halkos GE, Gkampoura E-C. Reviewing usage, potentials, and limitations of renewable energy sources. *Energies*. 2020;13(11):2906.
11. Fraenkel PL. Marine current turbines: moving from experimental test rigs to a commercial technology. In *ASME 2007 26th International Conference on Offshore Mechanics and Arctic Engineering*. American Society of Mechanical Engineers Digital Collection; 2007.
12. Segura E, Morales R, Somolinos JA, López A. Techno-economic challenges of tidal energy conversion systems: Current status and trends. *Renew Sustain Energy Rev*. 2017;77:536-550.
13. Lam W-H, Bhatia A. Folding tidal turbine as an innovative concept toward the new era of turbines. *Renew Sustain Energy Rev*. 2013;28:463-473.

14. Yin X, Zhao X. Sensorless maximum power extraction control of a hydrostatic tidal turbine based on adaptive extreme learning machine. *IEEE Trans Sustain Energy*. 2019;11(1):426-435.
15. Yin X, Zhang W, Jiang Z, Pan L. Data-driven multi-objective predictive control of offshore wind farm based on evolutionary optimization. *Renewable Energy*. 2020;160:974-986.
16. Yin X, Zhang W, Jiang Z, Pan L, Lei M. Adaptive backstepping control for maximizing marine current power generation based on uncertainty and disturbance estimation. *Int J Electr Power Energy Syst*. 2020;117:105329.
17. Clarke JA, Connor G, Grant A, Johnstone C, Ordonez Sanchez S. Contra-rotating marine current turbines: single point tethered floating system-stability and performance. In *8th European Wave and Tidal Energy Conference, EWTEC 2009*. 2009.
18. Liu P, Veitch B. Design and optimization for strength and integrity of tidal turbine rotor blades. *Energy*. 2012;46(1):393-404.
19. Gupta R, Biswas A, Sharma K. Comparative study of a three-bucket Savonius rotor with a combined three-bucket Savonius–three-bladed Darrieus rotor. *Renewable Energy*. 2008;33(9):1974-1981.
20. Sharma KK, Gupta R, Biswas A. Performance measurement of a two-stage two-bladed Savonius rotor. *Int J Renewable Energy Res*. 2014;4(1):115-121.
21. Mohamed M. Performance investigation of H-rotor Darrieus turbine with new airfoil shapes. *Energy*. 2012;47(1):522-530.
22. Prieto M, Montanes E, Menendez O. Power plant condenser performance forecasting using a non-fully connected artificial neural network. *Energy*. 2001;26(1):65-79.
23. Laín Beatove S, Osorio C. Simulation and evaluation of a straight-bladed Darrieus-type cross flow marine turbine; 2010.
24. Lee T-L. Back-propagation neural network for long-term tidal predictions. *Ocean Eng*. 2004;31(2):225-238.
25. Supharatid S. Tidal-level forecasting and filtering by neural network model. *Coastal Eng J*. 2003;45(01):119-137.
26. Deo M, Chaudhari G. Tide prediction using neural networks. *Computer-Aided Civil Infrastruct Eng*. 1998;13(2):113-120.
27. Yin X, Zhao X. Big data driven multi-objective predictions for offshore wind farm based on machine learning algorithms. *Energy*. 2019;186:115704.
28. Wu J, Liu C. Short-term wind power prediction based on empirical mode decomposition and extreme learning machine. In *2016 5th International Conference on Environment, Materials, Chemistry and Power Electronics*. Atlantis Press; 2016.
29. Tian Z, Wang G, Li S, Wang Y, Wang X. Artificial bee colony algorithm–optimized error minimized extreme learning machine and its application in short-term wind speed prediction. *Wind Eng*. 2019;43(3):263-276.
30. Tian Z, Li S, Wang Y. A prediction approach using ensemble empirical mode decomposition-permutation entropy and regularized extreme learning machine for short-term wind speed. *Wind Energy*. 2020;23(2):177-206.
31. Huang G-B, Zhu Q-Y, Siew C-K. Extreme learning machine: a new learning scheme of feedforward neural networks. In *2004 IEEE international joint conference on neural networks (IEEE Cat. No. 04CH37541)*. IEEE; 2004.
32. Ghouti L. Mobility prediction in mobile ad hoc networks using neural learning machines. *Simul Model Pract Theory*. 2016;66:104-121.
33. Nian R, He B, Zheng B, et al. Extreme learning machine towards dynamic model hypothesis in fish ethology research. *Neurocomputing*. 2014;128:273-284.
34. Wang DD, Wang R, Yan H. Fast prediction of protein–protein interaction sites based on extreme learning machines. *Neurocomputing*. 2014;128:258-266.
35. Wang X, Han M. Online sequential extreme learning machine with kernels for nonstationary time series prediction. *Neurocomputing*. 2014;145:90-97.
36. Wong PK, Wong KI, Vong CM, Cheung CS. Modeling and optimization of biodiesel engine performance using kernel-based extreme learning machine and cuckoo search. *Renewable Energy*. 2015;74:640-647.
37. Yu Q, Miche Y, Séverin E, Lendasse A. Bankruptcy prediction using extreme learning machine and financial expertise. *Neurocomputing*. 2014;128:296-302.
38. Vapnik V. *The nature of statistical learning theory*. Springer science and business media; 2013.
39. Laín S, et al. Design optimization of a vertical axis water turbine with CFD. *Alternative energies*. Springer; 2013:113-139.
40. Huang G, Huang GB, Song S, You K. Trends in extreme learning machines: A review. *Neural Networks*. 2015;61:32-48.
41. Tavares LD, Saldanha RR, Vieira DA. Extreme learning machine with parallel layer perceptrons. *Neurocomputing*. 2015;166:164-171.
42. Zhongda T, Shujiang L, Yanhong W, Xiangdong W. Network traffic prediction method based on improved ABC algorithm optimized EM-ELM. *The Journal of China Universities of Posts and Telecommunications*. 2018;3:6.
43. Tian Z, Ren Y, Wang G. Short-term wind speed prediction based on improved PSO algorithm optimized EM-ELM. *Energy Sources, Part A: Recovery, Utilization Environ Effects*. 2019;41(1):26-46.
44. Tian Z, Wang G, Ren Y, Li S, Wang Y. An adaptive online sequential extreme learning machine for short-term wind speed prediction based on improved artificial bee colony algorithm. *Neural Network World*. 2018;28(3):191-212.
45. Arab Golarche A, Moghiman M, Javadi MalAbad SM. Numerical simulation of darrieus wind turbine Using 6DOF model to consider the effect of inertia and the fluid-solid interaction. *Modares. Mechanical Eng*. 2016;15(12):143-152.
46. Liang N-Y, Huang G-B, Saratchandran P, Sundararajan N. A fast and accurate online sequential learning algorithm for feedforward networks. *IEEE Trans Neural Networks*. 2006;17(6):1411-1423.
47. Tang J, Deng C, Huang G-B. Extreme learning machine for multilayer perceptron. *IEEE Trans Neural Netw Learn Syst*. 2015;27(4):809-821.
48. Huang G-B, Zhou H, Ding X, Zhang R. Extreme learning machine for regression and multiclass classification. *IEEE Trans Syst Man Cybernet Part B (Cybernetics)*. 2011;42(2):513-529.
49. Ghouti L, Sheltami TR, Alutaibi KS. Mobility prediction in mobile Ad Hoc networks using extreme learning machines. *Procedia Computer Science*. 2013;19:305–312.
50. Huang G-B, Zhu Q-Y, Siew C-K. Extreme learning machine: theory and applications. *Neurocomputing*. 2006;70(1–3):489-501.
51. Vapnik VN. Complete statistical theory of learning. *Automation and Remote Control*. 2019;80(11):1949-1975.
52. Vapnik V, Izmailov R. Rethinking statistical learning theory: learning using statistical invariants. *Mach Learn*. 2019;108(3):381-423.
53. Rajasekaran S, Gayathri S, Lee T-L. Support vector regression methodology for storm surge predictions. *Ocean Eng*. 2008;35(16):1578-1587.

54. Zhang L, Zhou W-D, Chang P-C, Yang J-W, Li F-Z. Iterated time series prediction with multiple support vector regression models. *Neurocomputing*. 2013;99:411-422.
55. Petković D, Arif M, Shamshirband S, Bani-Hani EH, Kiakojoori D. Sensorless estimation of wind speed by soft computing methodologies: a comparative study. *Informatika*. 2015;26(3):493-508.
56. Assareh E, Behrang MA, Assari MR, Ghanbarzadeh A. Application of PSO (particle swarm optimization) and GA (genetic algorithm) techniques on demand estimation of oil in Iran. *Energy*. 2010;35(12):5223-5229.
57. Ji Y, Sun S. Multitask multiclass support vector machines: model and experiments. *Pattern Recogn*. 2013;46(3):914-924.
58. Wang F, Li D. A method of parameters selection with higher accuracy for SVM. In *2012 IEEE Fifth International Conference on Advanced Computational Intelligence (ICACI)*. IEEE; 2012.
59. Wei Z, Tao T, ZhuoShu D, Zio E. A dynamic particle filter-support vector regression method for reliability prediction. *Reliability Eng System Safety*. 2013;119:109-116.
60. Yang X-S. Multiobjective firefly algorithm for continuous optimization. *Eng Computers*. 2013;29(2):175-184.
61. Yang X-S. *Engineering optimization: an introduction with meta-heuristic applications*. John Wiley and Sons; 2010.
62. Yang X-S. *Introduction to computational mathematics*. World Scientific Publishing Company; 2014.
63. Agarwal S, Singh AP, Anand N. Evaluation performance study of Firefly algorithm, particle swarm optimization and artificial bee colony algorithm for non-linear mathematical optimization functions. In *2013 Fourth International Conference on Computing, Communications and Networking Technologies (ICCCNT)*. IEEE; 2013.
64. Ghazvinei P, Shamshirband S, Motamedi S, Hassanpour Darvishi H, Salwana E. Performance investigation of the dam intake physical hydraulic model using Support Vector Machine with a discrete wavelet transform algorithm. *Computers and Electronics in Agriculture*. 2017;140:48-57.
65. Taherei Ghazvinei P, Hassanpour Darvishi H, Mosavi A, et al. Sugarcane growth prediction based on meteorological parameters using extreme learning machine and artificial neural network. *Eng Appl Computat Fluid Mechanics*. 2018;12(1):738-749.

How to cite this article: Band SS, Taherei Ghazvinei P, bin Wan Yusof K, Hossein Ahmadi M, Nabipour N, Chau K-W. Evaluation of the accuracy of soft computing learning algorithms in performance prediction of tidal turbine. *Energy Sci Eng*. 2021;9:633–644. <https://doi.org/10.1002/ese3.849>